

Vibrational response functions for multidimensional electronic spectroscopy: from Duschinsky rotations to multimode squeezed coherent states

Frank Ernesto Quintela Rodriguez
Università di Modena e Reggio Emilia, I-41125 Modena, Italy

Filippo Troiani*

Centro S3, CNR-Istituto di Nanoscienze, I-41125 Modena, Italy and

*Author to whom correspondence should be addressed: filippo.troiani@nano.cnr.it

(Dated: July 31, 2023)

Multidimensional spectroscopy unveils the interplay of nuclear and electronic dynamics, which characterizes the ultrafast dynamics of various molecular and solid-state systems. In a class of models widely used for the simulation of such dynamics, field-induced transitions between electronic states result in linear transformations (Duschinsky rotations) between the normal coordinates of the vibrational modes. Here we present an approach for the calculation of the response functions, based on the explicit derivation of the vibrational state. This can be shown to coincide with a multimode squeezed coherent state, whose expression we derive within a quantum-optical formalism, and specifically by the sequential application to the initial state of rotation, displacement and squeeze operators. The proposed approach potentially simplifies the numerical derivation of the response functions, avoiding the time integration of the Schrödinger equation, the Hamiltonian diagonalization, and the sum over infinite vibronic pathways. Besides, it quantitatively substantiates in the considered models the intuitive interpretation of the response functions in terms of the vibrational wave packet dynamics.

I. INTRODUCTION

Coherent multidimensional spectroscopy employs ultra-short laser pulses to probe the photo-physical dynamics in the femtosecond regime [1, 2]. The dependence of the observed polarization on the time delays between the pulses allows one to correlate the system's resonant frequencies and to discriminate distinctive features in the quantum dynamics [3, 4]. This technique has been widely applied to the study of diverse ultrafast physical processes, including, among others [5–7], charge separation [8], internal conversion [9], generation of polaron-pairs [10], and electron transfer [11, 12]. However, the interpretation of the multidimensional spectra is not immediate, and requires the aid of numerical simulations. These can complement the observable quantities with information on the potential energy surfaces (PESs) [13, 14] and, where needed, on the non-adiabatic couplings between electronic and nuclear degrees of freedom [15–17].

In order to simulate the multidimensional spectra, the systems can typically be modelled by a few electronic states, coupled to a set of independent harmonic oscillators. These are derived from the normal mode analysis of the PESs, performed within electronic structure calculations [18]. A full *ab initio* simulation of the spectra becomes in fact impractical as the size of the system increases and contributions from highly excited-states show up in the measured signal [19–21]. Model Hamiltonians that are quadratic in the momentum and coordinate operators, usually referred to as generalized Brownian oscillator models [3, 22, 23], account for the dominant (lower-order) contributions to the interaction potentials and have been extensively used in the simulation of experiments [24–26]. In adiabatic models, the vibrational

and electronic degrees of freedom factorize at the level of eigenstates [27–30], but can mix in the dynamics triggered by the laser pulses. In particular, in the Franck-Condon approximation, the laser pulses induce transitions between electronic states and simultaneously launch vibrational wave packets in the excited-state PES. Here they freely propagate during the time delays, giving rise to a modulation of the multidimensional electronic spectra. Specific features of such modulation can be typically traced back to the displacement of the equilibrium position of the PESs [3], to their electronic-state dependent curvature [31], and to the Duschinsky multi-mode mixing [32].

These Hamiltonian parameters contribute to the physical and spectral features in many different ways. It is known that a temperature dependence of the absorption line shape results from a difference between the ground and excited state vibrational frequencies [31]. In 2D spectroscopy, the electronic-state dependent frequencies can be used to unambiguously separate signals from excited and ground-state wave-packets [33]. Large differences in the curvatures of the PESs are also a notable feature of molecular photoswitches, which are currently studied by a wide variety of potential applications in nanotechnology [34, 35]. The Duschinsky mixing of normal modes can affect the transition rates for electron transfer [36, 37], internal conversion [38] and fluorescence rates [39, 40], as well as producing the cooling of the vibrational population in the excited state [41]. Their spectral signatures have been resolved by transient-absorption measurements [42], electronic-vibrational spectroscopy [43, 44], and 2D electronic spectroscopy [23].

Despite the simplifications introduced in the harmonic model, the calculation of the response functions might

turn out to be complicated, due to the inherent multi-level and multi-mode mixing present in the model. Exact analytical results for the linear response have been obtained from the quadratic propagator derived in the Feynman's path integral formulation [45]. Arbitrary orders of the nonlinear response can in principle be calculated from the known eigenstates of the harmonic model, but even there technical complications arise from the calculation of the Franck-Condon factors and from the need to include, in principle, an infinite number of vibronic pathways [46, 47]. Analytical calculations of the nonlinear response follow the cumulant expansion of the energy gap operator between electronic states. The exact third-order response is known for the two-level system with uniform PES curvatures and no Duschinsky mixing [3], and has been extended to multi-levels systems coupling an arbitrary system Hamiltonian to a harmonic bath [48, 49]. This is possible because quantum correlation functions beyond the second order vanish when the energy gap follows a Gaussian statistics, so that the truncation of the expansion at second order is exact. However, a non-uniform PES curvature and the Duschinsky mixing introduce non-Gaussian fluctuations, requiring that higher-order cumulants be taken into account [23, 50, 51]. The third-order response functions for harmonic oscillators with non-uniform PES curvatures have been calculated in the third-order cumulant expansion [31], and later extended by using the link between classical and quantum correlation functions [23]. Alternative numerical strategies are based on the integration of the master equation, for example within the Lindblad or Redfield theories [52–55], on the hierarchical equations of motion [56] or an approximate dynamics [57].

Here we follow a different route in the calculation of the vibrational response functions, which allows the calculation of arbitrary-order contributions in systems with arbitrary numbers of electronic levels. The approach is based on the explicit derivation of the vibrational state corresponding to each electronic pathways, *i.e.* to each sequence of electronic states, resulting from the laser-induced transitions. Besides providing the explicit expression of the vibrational states and a clear physical picture underlying the vibrational-induced modulation of the response functions, this approach does not require the counting over all the vibronic eigenstates of the full Hamiltonian, and thus circumvents the calculation of the Franck-Condon factors. The presented derivation employs a quantum optics formalism, and specifically the decomposition of the time-evolution generated by the vibrational Hamiltonian in terms of the rotation, displacement and squeeze operators [58–61]. From this decomposition it follows that the squeezed-coherent character of the vibrational state is preserved throughout its time evolution. This is particularly relevant, because the vibrational ground state is a particular case of a squeezed coherent state, and coherent states form an over-complete basis, in terms of which any initial state can be decomposed.

These results generalize those obtained along the same lines for the linearly displaced harmonic oscillator model, where the electronic-state dependence of the vibrational frequencies and mode mixing are not present [62]. While in that case closed analytical expressions could be derived for the vibrational response functions, here we provide iterative solutions for the quantities that define the multimode squeezed coherent states. The approach is applied for illustrative purposes to systems with two electronic levels and up to two vibrational modes. These examples clearly and intuitively show the connection between the dynamics of the vibrational wave packet(s) and the time dependence of the vibrational response functions.

The remainder of the paper is organized as follows. In Sect. II we introduce the approach by discussing the case of a single vibrational mode, with electronic-state dependent frequency. Section III presents the generalization of these results to the multimode case, where the mixing between the modes results from Duschinsky rotations. In Sect. IV we draw our conclusions. Background information is reported in Appendix B and C for the single- and multi-mode cases, respectively.

II. SINGLE VIBRATIONAL MODE WITH ELECTRONIC-STATE DEPENDENT FREQUENCY

In order to illustrate the procedure more smoothly, we start by discussing the simpler case of a single vibrational mode. The more general multimode case requires mathematically nontrivial, but conceptually straightforward, generalizations of the steps discussed in the present Section, and the inclusion of the Duschinsky rotations. These generalizations are discussed in the following Section.

A. Definition of the model and of the approach

The considered model consists of N_e electronic levels and a vibrational mode. This is specifically given by a harmonic oscillator, whose origin and frequency depend on the electronic state. The corresponding Hamiltonian reads:

$$H = \sum_{\lambda=0}^{N_e} |\lambda\rangle\langle\lambda| \otimes (\epsilon_\lambda + H_{v,\lambda}), \quad (1)$$

where the vibrational components $H_{v,\lambda}$ are given by:

$$H_{v,\lambda} = \omega_\lambda [(a_\lambda^\dagger + \delta_\lambda)(a_\lambda + \delta_\lambda) + 1/2]. \quad (2)$$

The displacements δ_λ are assumed to be real. Without loss of generality, we set for the ground state $\delta_0 = 0$. Given the dependence of the vibrational frequency on

the electronic state, and thus on the pathway that specifies the contribution to the response function, the constant term $1/2$ in $H_{v,\lambda}$ cannot be neglected. As to the Hamiltonian eigenstates, these can always be written in a factorized form, given by the product of the electronic state $|\lambda\rangle$, and of the Fock state $|n_\lambda\rangle$, where $H_{v,\lambda}|n_\lambda\rangle = (\hbar\omega_\lambda + 1/2)|n_\lambda\rangle$.

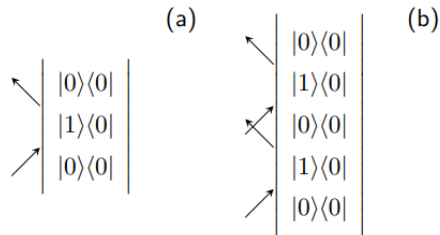


FIG. 1. Double-sided Feynman diagrams corresponding to the (a) first- and (b) third-order response functions of a system with two electronic levels, where the interactions with the field all occur on the left side. The third-order diagram can be related to the non-rephasing part of the ground-state bleaching contribution ($\lambda_1 = 1$, $\lambda_2 = 0$, and $\lambda_3 = 1$). As required in the present approach, the diagrams only specify the electronic pathway p_e .

The response functions that are used in the simulation of multidimensional spectroscopy correspond to multi-time correlations function. In the following, we specifically refer to first- and third-order response functions, which are given, respectively, by [1, 3]:

$$R^{(1)} = (i/\hbar)\langle\mu(t_1), [\mu, \rho_0]\rangle, \quad (3)$$

and

$$R^{(3)} = (i/\hbar)^3\langle\mu(t_{123}), [\mu(t_{12}), [\mu(t_1), [\mu, \rho_0]]]\rangle, \quad (4)$$

where $t_{123} \equiv t_1 + t_2 + t_3$ and $t_{ij} \equiv t_i + t_j$. The density operator ρ_0 defines the initial state of the system, which is hereafter assumed to coincide with its ground state, while $\mu(t) = U^\dagger(t)\mu U(t)$ is the dipole operator in the Heisenberg representation, with $U(t) = e^{-iHt/\hbar}$ and $\mu \equiv \mu(0)$. Within the Franck-Condon approximation, the system undergoes sudden transitions between electronic states, induced by the electric field, that leave the vibrational state unchanged. Correspondingly, the dipole operator coincides with the identity in the vibrational space.

The response functions can be written as the sum over a number of contributions, one for each pathway [1, 3]. In particular, we refer hereafter to the pathways (double sided Feynman diagrams) where the interactions with the field all occur on the left: all other cases can be derived from this one by suitably redefining the waiting times (see Appendix A and Refs. 63 and 64). For an Hamiltonian such as the one defined by Eqs. (1-2), there are in principle infinite vibronic pathways p , each one corresponding to a different sequence of transitions between

electron-vibrational eigenstates $|\lambda, n_\lambda\rangle$:

$$p : |\lambda_1, n_{\lambda_1}\rangle \longrightarrow |\lambda_2, n_{\lambda_2}\rangle \cdots \longrightarrow |\lambda_M, n_{\lambda_M}\rangle. \quad (5)$$

Here we follow an alternative approach, allowed by the adiabatic character of the coupling between electronic and vibrational degrees of freedom [62]. This consists in factorizing — for each electronic pathway p_e — the response function into the product of an electronic and a vibrational component,

$$R_\Lambda^{(M)}(\mathbf{t}) = R_\Lambda^{(e,M)}(\mathbf{t}) R_\Lambda^{(v,M)}(\mathbf{t}) \quad [\mathbf{t} = (t_1, \dots, t_M)], \quad (6)$$

and deriving the time evolution of the latter component, being p_e [or, equivalently, $\Lambda = (\lambda_1, \dots, \lambda_M)$] defined exclusively by the sequence of electronic states

$$p_e : |\lambda_1\rangle \longrightarrow |\lambda_2\rangle \cdots \longrightarrow |\lambda_M\rangle. \quad (7)$$

Not including any dependence on the vibrational quantum numbers n_{λ_k} , the electronic pathways (p_e) are infinitely less numerous than the vibronic ones (p). The role played by the vibrational degrees of freedom is entirely captured by the electronic-pathway dependent evolution of the vibrational state. This is generated by an Hamiltonian that is piecewise constant:

$$|\psi_{ket,\Lambda}\rangle = e^{-iH_{v,\lambda_M}t_M/\hbar} \cdots e^{-iH_{v,\lambda_1}t_1/\hbar}|0_0\rangle, \quad (8)$$

being $|0_0\rangle$ the ground vibrational state of the ground state harmonic oscillator Hamiltonian $H_{v,0}$. The vibrational component of the response function is given by the overlap between these two states,

$$R_\Lambda^{(v,M)}(\mathbf{t}) = \langle\psi_{bra}|\psi_{ket,\Lambda}\rangle \quad (9)$$

where the former one is given by the ground vibrational state, $|\psi_{bra}\rangle = e^{-i\omega_0 \sum_{k=1}^M t_k/2}|0_0\rangle$. The p_e -dependent vibrational state $|\psi_{ket,\Lambda}\rangle$ is given, for the present Hamiltonian, by a squeezed coherent state, and can thus be specified by one real and two complex numbers.

B. Rotation, displacement, and squeeze operators

If the harmonic oscillator is initialized in a squeezed coherent state, it remains in a squeezed coherent state at all times. This results from the fact that each time-evolution operator $e^{-iH_{v,\lambda}t/\hbar}$ can be written as the product of a squeeze, a displacement, and a rotation operator [32, 58], and that the application of each of these operators to a squeezed coherent state gives rise to another squeezed coherent state.

1. Definition of the operators

For the reader's convenience, we report hereafter the definitions of these operators [65, 66]. The rotation operator can be expressed as an exponential function of the

number operator $a^\dagger a$:

$$R(\phi) = \exp(i\phi a^\dagger a), \quad (10)$$

where ϕ is real and defines the rotation angle. The time evolution operator generated by the undisplaced oscillator Hamiltonian $H_{v,0}$ corresponds to a rotation operator with $\phi = -\omega_0 t$, multiplied by a phase factor $e^{-i\omega_0 t/2}$.

Also the displacement operator can be written as an exponential function of the creation and annihilation operators, and specifically as:

$$D(\beta) = \exp(\beta a^\dagger - \beta^* a), \quad (11)$$

where β is a complex number. In the absence of a frequency change, *i.e.* if $\omega_\lambda = \omega_0$ for any λ , the time evolution operator $e^{-iH_{v,\lambda}t/\hbar}$ can be written as a combination of a rotation and two displacement operators [62], times a phase factor $e^{-i\omega_0 t/2}$.

Finally, the squeeze operator is given by an exponential function of the creation and annihilation operators squared:

$$S(w) = \exp\left\{\frac{1}{2}\left[w^* a^2 - w (a^\dagger)^2\right]\right\}, \quad (12)$$

where w is a complex number. The main properties of the rotation, displacement, and squeeze operators are reported in Appendix B.

2. Definition and transformation of the squeezed coherent states

The relevant vibrational states are here represented by the so-called *squeezed coherent states*. These are obtained by sequentially applying a squeeze and a displacement operator to the vacuum state [65, 66]

$$|\alpha, z\rangle \equiv D(\alpha) S(z) |0\rangle. \quad (13)$$

By exploiting the commutation relations between the rotation, squeeze, and displacement operators, one can show that their application to a squeezed coherent state gives rise to another squeezed coherent state (see Appendix B). In particular, the application of the rotation operator to a squeezed coherent state modifies it as follows:

$$R(\phi) (e^{i\zeta} |\alpha, z\rangle) = e^{i\zeta'} |\alpha', z'\rangle, \quad (14)$$

where the relation between the initial and final states is given by:

$$\alpha' = \alpha e^{i\phi}, \quad z' = z e^{2i\phi}, \quad \zeta' = \zeta. \quad (15)$$

The application of the displacement operator modifies a squeezed coherent state according to the equation:

$$D(\beta) (e^{i\zeta} |\alpha, z\rangle) = e^{i\zeta'} |\alpha', z'\rangle, \quad (16)$$

where initial and final states are related by:

$$\alpha' = \alpha + \beta, \quad z' = z, \quad \zeta' = \zeta - i(\beta\alpha^* - \beta^*\alpha)/2. \quad (17)$$

Finally, the application of the squeeze operator to a squeezed coherent state modifies it as follows:

$$S(w) (e^{i\zeta} |\alpha, z\rangle) = e^{i\zeta'} |\alpha', z'\rangle, \quad (18)$$

where the relation between initial and final states is defined by the equations:

$$\begin{aligned} \alpha' &= \alpha \cosh |w| - \alpha^* e^{i\theta_w} \sinh |w|, \\ e^{i\zeta'} &= e^{i\zeta} \left(\frac{1 + t_w t_z^*}{|1 + t_w t_z^*|} \right)^{1/2}. \end{aligned} \quad (19)$$

Here, $z = |z| e^{i\theta_z}$, t_z is given by the expression

$$t_z \equiv e^{i\theta_z} \tanh |z|, \quad (20)$$

and an analogous relation applies to w and t_w . Consistently with the above definitions, the parameter z' is given by the equation

$$t_{z'} = \frac{t_z + t_w}{1 + t_z t_w^*}, \quad (21)$$

through the relations $|z'| = \operatorname{atanh} |t_{z'}|$ and $e^{i\theta_{z'}} = t_{z'}/|t_{z'}|$.

C. Reduction of the time evolution to squeezing, displacements and rotations

The vibrational time evolution operator corresponding to each time interval t_k can be decomposed into the product of rotation, displacement, and squeeze operators [32, 58]. One possible decomposition, which can be generalized to the multimode case, is given by the expression

$$\begin{aligned} U_k(t_k) &\equiv e^{-iH_{v,\lambda_k} t_k/\hbar} = e^{-\omega_{\lambda_k} t_k/2} S(x_{\lambda_k} - x_0) \\ &D(-\delta_{\lambda_k}) R(-\omega_{\lambda_k} t_k) D(\delta_{\lambda_k}) S(x_0 - x_{\lambda_k}). \end{aligned} \quad (22)$$

Here $x_\lambda \equiv \frac{1}{2} \ln \omega_\lambda$, with adimensional ω_λ , obtained by dividing each angular frequency by a common reference value. As a result, and in view of the equations reported in the previous Subsection, a squeezed coherent state whose dynamics is generated by an Hamiltonian $H_{v,\lambda}$ evolves into another squeezed coherent state, and can thus be identified by the two complex numbers α and z , plus the global phase ζ .

1. Stepwise derivation of the final vibrational states

The time evolution of the vibrational state is generated by a Hamiltonian that is constant during each time interval t_k , and changes from one interval to the other [Eq. (8)]. We call $e^{i\zeta_{k,i}} |\alpha_{k,i}, z_{k,i}\rangle$ and $e^{i\zeta_{k,f}} |\alpha_{k,f}, z_{k,f}\rangle$

the squeezed coherent state respectively at the beginning and at the end of t_k . The final state for each time interval coincides with the initial state for the following one:

$$e^{i\zeta_{k,i}}|\alpha_{k,i}, z_{k,i}\rangle \equiv e^{i\zeta_{k-1,f}}|\alpha_{k-1,f}, z_{k-1,f}\rangle. \quad (23)$$

In order to derive the vibrational state at the end of the time interval, one can first reduce the time evolution operator $e^{-iH_{v,\lambda_k}t_k/\hbar}$ to the product of squeeze, displacement, and rotation operators [Eq. (22)], and then sequentially apply such operators to the vibrational state. The resulting intermediate states, referred to as $e^{i\zeta_{k,l}}|\alpha_{k,l}, z_{k,l}\rangle$ (with $l = 1, \dots, 5$), are derived as follows:

1. The first intermediate state is obtained by applying the squeeze operator, and thus of Eqs. (19-21), with $w = \frac{1}{2} \ln(\omega_0/\omega_{\lambda_k})$. The states before and after such application are specified by $(\alpha, z, \zeta) = (\alpha_{k,i}, z_{k,i}, \zeta_{k,i})$ and $(\alpha', z', \zeta') = (\alpha_{k,1}, z_{k,1}, \zeta_{k,1})$.
2. The second intermediate state is obtained by applying a displacement operator, and thus of Eq. (17), with $\beta = \delta_{\lambda_k}$. The states before and after such application are specified by $(\alpha, z, \zeta) = (\alpha_{k,1}, z_{k,1}, \zeta_{k,1})$ and $(\alpha', z', \zeta') = (\alpha_{k,2}, z_{k,2}, \zeta_{k,2})$.
3. The third intermediate state results from the application of a rotation operator [Eq. (14)], with $\phi = -\omega_{\lambda_k}t_k$. The states before and after such application are specified by $(\alpha, z, \zeta) = (\alpha_{k,2}, z_{k,2}, \zeta_{k,2})$ and $(\alpha', z', \zeta') = (\alpha_{k,3}, z_{k,3}, \zeta_{k,3})$.
4. The fourth intermediate state is obtained by applying a displacement operator [Eq. (17)], with $\beta = -\delta_{\lambda_k}$. The states before and after such application are specified by $(\alpha, z, \zeta) = (\alpha_{k,3}, z_{k,3}, \zeta_{k,3})$ and $(\alpha', z', \zeta') = (\alpha_{k,4}, z_{k,4}, \zeta_{k,4})$.
5. The fifth state squeezed coherent state results from the application of a squeeze operators, and thus of Eqs. (19-21), with $w = \frac{1}{2} \ln(\omega_{\lambda_k}/\omega_0)$. The states before and after such application are specified by $(\alpha, z, \zeta) = (\alpha_{k,4}, z_{k,4}, \zeta_{k,4})$, and $(\alpha', z', \zeta') = (\alpha_{k,5}, z_{k,5}, \zeta_{k,5})$.

The vibrational state at the end of the waiting time t_k is then given by $\alpha_{k,f} = \alpha_{k,5}$, $z_{k,f} = z_{k,5}$, and $\zeta_{k,f} = \zeta_{k,5} - \omega_{\lambda_k}t_k/2$. We stress that the $e^{i\zeta_{k,l}}|\alpha_{k,l}, z_{k,l}\rangle$ are fictitious intermediate states: the vibrational state does not go through these states during its time evolution, but it does coincide with $e^{i\zeta_{k,i}}|\alpha_{k,i}, z_{k,i}\rangle$ and $e^{i\zeta_{k,f}}|\alpha_{k,f}, z_{k,f}\rangle$, respectively at the beginning and at the end of the waiting time t_k .

D. Vibrational response functions

The vibrational component of the M -th order response function is given by the overlap between the final vibrational state $e^{i\zeta}|\alpha, z\rangle$, corresponding to the state at the

end of the M -th waiting time, and the initial vibrational state, coinciding with the ground state of $H_{v,0}$:

$$R_{\Lambda}^{(v,M)}(\mathbf{t}) = \langle \psi_{bra} | \psi_{ket,\Lambda} \rangle = e^{i\zeta} \langle 0 | \alpha, z \rangle = \frac{e^{i\zeta}}{\sqrt{\cosh |z|}} \exp \left\{ -\frac{1}{2} [|\alpha|^2 - t_z(\alpha^*)^2] \right\}, \quad (24)$$

where t_z is given by Eq. (20), and the squeezed coherent state is given by $\alpha = \alpha_{M,f}$, $z = z_{M,f}$, and $\zeta = \zeta_{M,f} + \omega_0 \sum_{k=1}^M t_k/2$.

If the initial state of the vibrational mode does not coincide with the ground state of $H_{v,0}$, but with a generic squeezed coherent state, $|\alpha_0, z_0\rangle$, the above procedure for the derivation of the vibrational response function has to be slightly modified, by adding to the sequence a squeeze, a rotation, and a displacement operator:

$$R_{\Lambda}^{(v,M)}(\mathbf{t}) = \langle \psi_{bra} | \psi_{ket,\Lambda} \rangle = e^{i\phi_0/2} \langle 0 | \psi'_{ket,\Lambda} \rangle, \quad (25)$$

where $\phi_0 = \omega_0 \sum_{j=1}^M t_j$ and the effective ket state reads:

$$|\psi'_{ket,\Lambda}\rangle = S(-z_0) D(-\alpha_0) R(\phi_0) \left(e^{-iH_{v,\lambda_M}t_M/\hbar} \dots e^{-iH_{v,\lambda_1}t_1/\hbar} \right) |\alpha_0, z_0\rangle. \quad (26)$$

E. Application to some representative case

For simplicity, we apply the above approach to the calculation of the first- and third-order response functions of a two-level system ($N_e = 2$). The double-sided Feynman diagrams that are relevant for the first- and third-order response functions and where all the interactions with the field occur on the left (ket) are shown in Fig. 1.

1. First-order response functions

In the linear case ($M = 1$), the electronic component of the response function is given by [1]

$$R_{\Lambda}^{(e,1)}(t_1) = i|\mu_{01}|^2 e^{-i\epsilon_1 t_1/\hbar} e^{-(\gamma+\Gamma/2)t_1}, \quad (27)$$

where $\epsilon_0 = 0$, $\Lambda = (1)$, and γ (Γ) is the dephasing (relaxation) rate. The effective inclusion of dephasing and relaxation into a closed-system approach is based on some specific assumption: first, that dephasing results in the (exponential) decay of the coherences generated by the electric field, and doesn't give rise to a transfer between one coherence and the other [?]; second, that the pathways generated by the relaxation process through population transfer can be neglected.

The vibrational response function is obtained by applying the equations reported above in Subsections II B-II C, and specifically for $M = 1$ and $\lambda_1 = 1$. In fact, these equations provide the time evolution of the vibrational state, *i.e.* the dependence on t_1 of the state

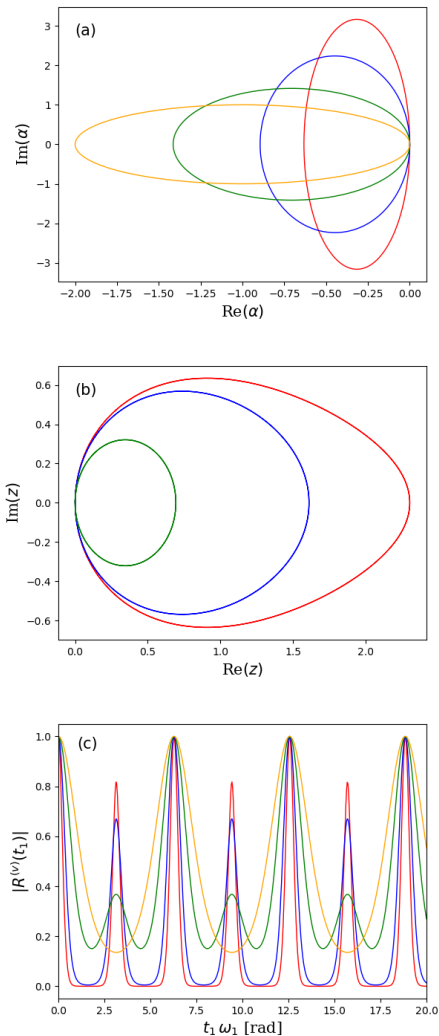


FIG. 2. Trajectory described by the squeezed coherent state, defined by the values of the complex numbers (a) α and (b) z . Please note that for visualization purposes, the scales of the two axes are different. (c) Time dependence of the vibrational component of the linear response function ($M = 1$). The curves in the three panels are obtained for a same value of the displacement $\delta_1 = 1$, and for different values of the ratio ω_1/ω_0 between ground- and excited-state vibrational frequencies: 10 (red), 5 (blue), 2 (green), 1 (orange).

$|\psi_{ket,\Lambda}\rangle = e^{i\zeta}|\alpha, z\rangle$, whose overlap with the initial state $|0_0\rangle$ gives the vibrational response function [Eq. (9)]. The global phase ζ is specific of each electronic pathway p_e , and thus determines the algebraic sum of contributions resulting from different pathways. While focusing on a single pathway, the discussion can be limited to the time evolution of the two complex numbers, α and z .

In Fig. 2(a), we plot the trajectory described by α in the plane [$\alpha_r \equiv \text{Re}(\alpha)$, $\alpha_i \equiv \text{Im}(\alpha)$], as a function of the waiting time t_1 . We note that the real and imaginary parts of α coincide with the expectation values of the quadrature operators $X_1 = (a + a^\dagger)/2$ and $X_2 =$

$(a - a^\dagger)/2i$, respectively. In the particular case where the electronic excitation implies a displacement of the oscillator, but not a change in the vibrational frequency ($\omega_1 = \omega_0$), α describes a circle with radius $|\delta_1|$, centered in $(-\delta_1, 0)$ [62]. For increasing values of ω_1/ω_0 , the trajectories described by the parameter α are increasingly elongated along α_i . As results from Eq. (22), the time dependence of α is periodic, with a periodicity that depends on the excited-state vibrational frequency through the relation $\omega_1 t_1 = 2k\pi$. However, but the trajectory described in the (α_r, α_i) plane only depends on the displacement and on the ratio between the frequencies (the same applies to z , see below). The squeezing parameter z also describes a closed trajectory in the (z_r, z_i) plane, and specifically in the region $z_r \geq 0$ [Fig. 2(b)]. In particular, for $\omega_1 = \omega_0$ no squeezing occurs, and z remains identically zero. In the presence of an electronic-state dependence of the vibrational frequency, and specifically for $\omega_1 \neq \omega_0$, the trajectories described by z range from $z_r = 0$ to $z_r = \ln(\omega_1/\omega_0)$, the latter corresponding to a maximum squeezing along the X_1 direction.

The modulus of the vibrational response function corresponds to that of the overlap between $|\alpha, z\rangle$ and $|0\rangle$ [Eq. (24)]. Such overlap is always maximum for $t_1\omega_1 = 2k\pi$, where the final and initial vibrational states coincide. In the absence of squeezing, $R^{(v,1)p_e}(t_1)$ presents minima for $t_1\omega_1 = (2n+1)\pi$, where $|\alpha|$ is maximal and is given by $2|\delta_1|$. For decreasing values of ω_1/ω_0 , however, local maxima of increasing height appear at $t_1\omega_1 = (2n+1)\pi$, due to the decreasing distance between the the origin of the (α_r, α_i) plane and the second intersection with the α_r axis [Fig. 2(a)]. For $\omega_0 > \omega_1$ (not reported here), the trajectory of α is elongated along α_r , that of z is contained in the half plane $z_r < 0$, and the local maxima in the modulus of the vibrational response function are absent. All this shows a clear connection between the electronic-state dependent change of the vibrational frequency, the trajectory of the squeezed coherent state, and features observed in the response function.

2. Third-order response functions

For the third-order term ($M = 3$), we specifically consider the non-rephasing part of the ground-state bleaching contribution [$\lambda_1 = \lambda_3 = 1$ and $\lambda_2 = 0$, Fig. 1(b)]. The electronic part of the response function is given by [1]

$$R_\Lambda^{(e,3)}(\mathbf{t}) = -i|\mu_{01}|^4 e^{-i\epsilon_1(t_1+t_3)/\hbar} e^{-(\gamma+\Gamma/2)(t_1+t_3)} \quad (28)$$

where $\epsilon_0 = 0$, $\Lambda = (1, 0, 1)$, and γ (Γ) is the dephasing (relaxation) rate.

The parameters α and z are themselves functions of the three waiting times. For fixed values of two times, they describe closed trajectories as a function of the third time, similar to those shown above for the case of linear response functions. The dependence of $|\alpha|$ on the

first and third waiting times, for a fixed value of t_2 and decreasing values of ω_1/ω_0 , is reported in Fig. 3 [panels (a) to (f)]. The displayed time ranges are limited to $0 \leq t_k \omega_k \leq 2\pi$ because α is a periodic function of the waiting times (and so is z), being its dependence on t_k entirely contained in that of $R(-\omega_{\lambda_k} t_k)$ [Eq. (22)], which coincides with $R(-\omega_{\lambda_k} t_k + 2\pi)$. The comparison between the different panels shows qualitative changes as a function of the ratio between the ground- and excited-state frequencies: in particular, a single maximum shows up for $\omega_0 = \omega_1$ (a), while four local maxima appear for $\omega_1 \geq 2.5\omega_0$ (e,f). Qualitative changes with $\omega_0 = \omega_1$ also occur to the local minima, corresponding to the regions in the (t_1, t_3) plane where the final vibrational state is closer to the initial one.

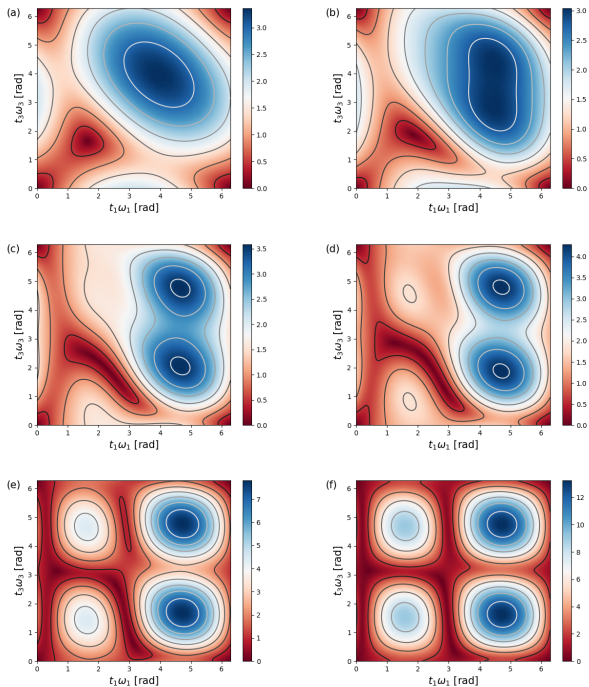


FIG. 3. Absolute value of α in the case $M = 3$, as a function of the waiting times t_1 and t_3 , and for $t_2\omega_0 = 1.5$ rad. Different panels correspond to different values of ω_1/ω_0 , and specifically: (a) 1, (b) 1.125, (c) 5/3, (d) 2, (e) 2.5, (f) 5. In all cases, the displacement is given by $\delta_1 = 1$.

Besides these specific features, which can vary for different values of t_2 , we would like to stress the clear correlation between the behavior of $|\alpha|$ and that of the response function (Fig. 4). In fact, this displays minima (maxima) in the same regions where $|\alpha|$ displays its maxima (minima), and undergoes the same changes as a function of the ratio ω_1/ω_0 between the vibrational frequencies corresponding to the excited and ground electronic states. Such correlation results from the identification of the response function with the overlap between the initial and the final vibrational states, $|0, 0\rangle$ and $e^{i\zeta}|\alpha, z\rangle$, dominated by the exponential dependence on α [Eq. (24)].

Though complicated by the presence of multiple waiting times, also these trends clearly show the connection between the vibrational response function and the dynamics of the vibrational wave packet.

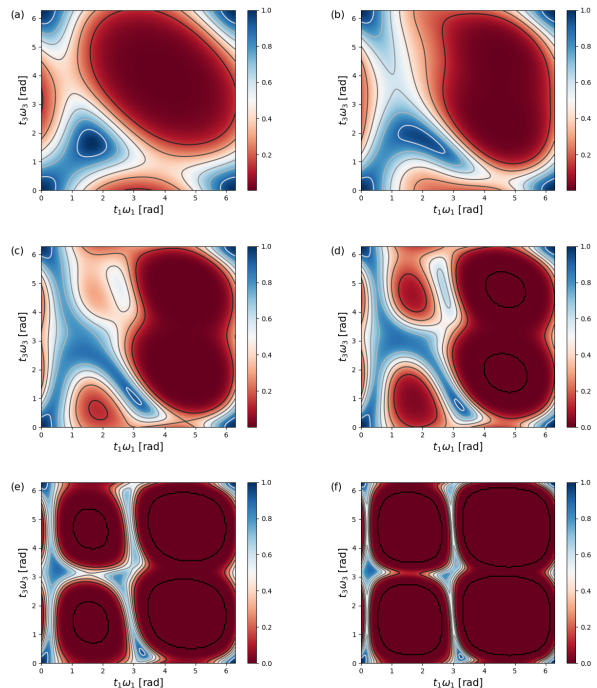


FIG. 4. Absolute value of the third-order vibrational response function $R^{(v)}$ in the case $M = 3$, as a function of the waiting times t_1 and t_3 , and for $t_2\omega_0 = 1.5$ rad. Different panels correspond to different values of ω_1/ω_0 , and specifically: (a) 1, (b) 1.125, (c) 5/3, (d) 2, (e) 2.5, (f) 5. In all cases, the displacement is given by $\delta_1 = 1$.

III. MULTIPLE VIBRATIONAL MODES WITH ELECTRONIC-STATE DEPENDENT FREQUENCY

In the presence of multiple modes, a change in the electronic state can also result in a rotation between the vibrational modes. The approach outlined so far can be generalized to deal with the multi-mode case, as shown in the following.

A. Definition of the model

The model system consists of N_e electronic levels and N vibrational modes. These are specifically given by a set of harmonic oscillators, whose frequency and origin depend on the electronic state. The corresponding

Hamiltonian reads:

$$H = \sum_{\lambda=0}^{N_e} |\lambda\rangle\langle\lambda| \otimes (\epsilon_\lambda + H_{v,\lambda}), \quad (29)$$

where the vibrational Hamiltonians $H_{v,\lambda}$ are given by:

$$H_{v,\lambda} = \sum_{j=1}^N \omega_{\lambda,j} (a_{\lambda,j}^\dagger a_{\lambda,j} + 1/2). \quad (30)$$

The modes corresponding to the electronic states λ and 0 (ground state) are assumed to be linearly related, and more specifically by the Duschinsky rotations [32, 61]:

$$\mathbf{q}_\lambda = U_\lambda \mathbf{q}_0 + \mathbf{d}_\lambda, \quad (31)$$

being U_λ the $N \times N$ orthogonal Duschinsky rotation matrix and \mathbf{d}_λ the displacement vector. The components of the vector \mathbf{q}_λ are the position operators $q_{\lambda,j}$ ($j = 1, \dots, N$), related to the creation and annihilation operators by the equations $q_{\lambda,j} = \sqrt{\hbar/(2\omega_{\lambda,j})}(a_{\lambda,j} + a_{\lambda,j}^\dagger)$. Correspondingly, the displacements of the position and annihilation (creation) operators are related by the equations $d_{\lambda,j} = \sqrt{2\hbar/\omega_{\lambda,j}} \delta_{\lambda,j}$.

As in the single-mode case, the time evolution of the vibrational state is induced by an Hamiltonian that is piecewise constant, and coincides at each time interval t_k with a H_{v,λ_k} , being λ_k an electronic state. As a result Eqs. (8-9) still apply, but $|\psi_{bra}\rangle$ and $|\psi_{ket,\Lambda}\rangle$ are now multi-mode vibrational states.

B. Rotation, displacement, and squeeze operators

In analogy with the single-mode case, we exploit the fact that a multi-mode squeezed coherent state evolves, under the effect of the Hamiltonians $H_{v,\lambda}$, into another squeezed coherent state. This again results from the fact that the time evolution operator can be decomposed into the product of rotation, squeeze, and displacement operators [32], and that each of these operators preserves the squeezed coherent character of the vibrational state.

1. Definition of the operators

The rotation, displacement, and squeeze operators can be generalized to the multimode case [59]. The rotation operator can be expressed as an exponential function of the creation and annihilation operators, according to the equation

$$R_N(\Phi) = \exp(i\tilde{a}^\dagger \Phi a). \quad (32)$$

Here Φ is a Hermitian matrix and $\tilde{a} = (a_1, \dots, a_{N_e})$ and $\tilde{a}^\dagger = (a_1^\dagger, \dots, a_{N_e}^\dagger)$ (the tilde represents the transposition of the $N_e \times 1$ matrixial operators a and a^\dagger). The time evolution operator generated by $H_{v,0}$ corresponds

to a rotation with a diagonal matrix Φ and nonzero elements $\Phi_{jj} = -\omega_{0,j} t$, multiplied by a phase factor $\prod_{j=1}^N e^{-i\omega_{0,j} t/2}$.

The displacement operator can also be written as an exponential function of the creation and annihilation operators:

$$D_N(B) = \exp(\tilde{B}a^\dagger - B^\dagger a), \quad (33)$$

where $\tilde{B} = (\beta_1, \dots, \beta_P)$ (the tilde and the dagger applied to a numerical matrix denote its simple and conjugate transpositions, respectively). One can easily verify that, unlike the rotation and squeeze operator (see below), the multimode displacement operator can always be written as the product of N single-mode displacement operators: $D_N(B) = \prod_{j=1}^N D(\beta_j)$.

Finally, the squeeze operator is given by an exponential function of a quadratic function of the creation and annihilation operators:

$$S_N(Z) = \exp\left[\frac{1}{2}(\tilde{a}Z^\dagger a - \tilde{a}^\dagger Z a^\dagger)\right], \quad (34)$$

where Z is a complex symmetric matrix. The main properties of the multi-mode rotation, squeeze, and displacement operators are recalled in Appendix C.

2. Definition and transformation of the squeezed coherent states

In analogy with the single-mode case, we identify the multi-mode squeezed coherent state with

$$|A, Z\rangle = D_N(A) S_N(Z) |0\rangle, \quad (35)$$

where $|0\rangle$ is the multi-mode vacuum state. If applied to a multi-mode squeezed coherent state, the operators $S_N(Z)$, $D_N(B)$, and $R_N(\Phi)$ generate another squeezed coherent state (see Appendix C for further details).

The application of the rotation operator to a squeezed coherent state induces the following transformation:

$$R_N(\Phi) (e^{i\zeta} |A, Z\rangle) = e^{i\zeta'} |A', Z'\rangle \quad (36)$$

where the parameters defining the initial and final states are related by

$$A' = e^{i\Phi} A, \quad Z' = e^{i\Phi} Z e^{i\tilde{\Phi}}, \quad \zeta' = \zeta \quad (37)$$

and $\tilde{\Phi}$ is the transpose of the matrix Φ .

The application of the displacement operator modifies a squeezed coherent state according to the equations

$$D_N(B) (e^{i\zeta} |A, Z\rangle) = e^{i\zeta'} |A', Z'\rangle, \quad (38)$$

where the parameters defining the initial and final states are related by

$$A' = A + B, \quad Z' = Z, \quad \zeta' = \zeta - i(A^\dagger B - B^\dagger A)/2. \quad (39)$$

The application of the squeeze operator modifies a squeezed coherent state according to the equations

$$S_N(W) (e^{i\zeta}|A, Z\rangle) = e^{i\zeta'}|A', Z'\rangle \quad (40)$$

where the transformed state is defined by

$$A' = \cosh|W|A - \sinh|W|e^{i\Theta_W}A^*, \quad (41)$$

where $W = |W|e^{i\Theta_W}$ is the polar decomposition of the $N \times N$ matrix W . The matrix Z' is determined by the equation

$$T_{Z'} = S_W^{-1}(T_W + T_Z)(I + T_W^\dagger T_Z)^{-1}\tilde{S}_W, \quad (42)$$

where $T_W \equiv \tanh|W|e^{i\Theta_W}$ (analogously for Z and Z') and $S_W \equiv \text{sech}|W|$. Finally, the phase factor results from

$$\zeta' = \zeta + \frac{1}{2}\text{Tr}(\Phi). \quad (43)$$

with

$$e^{i\Phi} = S_{Z'}^{-1}S_W(I + T_Z T_W^\dagger)^{-1}S_Z. \quad (44)$$

C. Reduction of the time evolution to squeezing, displacements and rotations

In analogy to what has been done in the single-mode case, the vibrational time evolution operator $e^{-iH_{v,\lambda_k}t_k/\hbar}$ can be written as the product of displacement, squeeze and rotation operators, according to the expression [32]:

$$U_k(t_k) = e^{-\sum_{j=1}^N \omega_{\lambda_k,j}t/2} S_N^\dagger(X_0) R_N^\dagger(\Phi_{\lambda_k}) S_N(X_{\lambda_k}) D_N^\dagger(\Delta_{\lambda_k}) R_N(\Phi'_{\lambda_k}) D_N(\Delta_{\lambda_k}) S_N^\dagger(X_{\lambda_k}) R_N(\Phi_{\lambda_k}) S_N(X_0). \quad (45)$$

Here the squeeze operators are defined by the matrix

$$X_\lambda = \frac{1}{2} \text{diag}(\ln \omega_{\lambda,1}, \dots, \ln \omega_{\lambda,N}) \quad (46)$$

and the displacement operators are defined by the vector

$$\tilde{\Delta}_\lambda = (\delta_{\lambda,1}, \dots, \delta_{\lambda,N}). \quad (47)$$

As to the rotation operators, the first and last ones are defined by the matrix

$$\Phi_\lambda = -i \ln U_\lambda \quad (48)$$

while the second rotation is defined by the diagonal matrix

$$\Phi'_\lambda = -t_k \text{diag}(\omega_{\lambda,1}, \dots, \omega_{\lambda,N}). \quad (49)$$

If there is no mixing between the modes ($\Phi_{\lambda_k} = 0$), $U_k(t_k)$ is reduced to the product of N single-mode time evolution operators, whose expression is given in Eq. (22).

1. Stepwise derivation of the final vibrational states

As in the single-mode case, the time evolution of the vibrational state is generated by a Hamiltonian that is constant during each time interval t_k , and changes from one interval to the other [Eq. (8)]. We call $e^{i\zeta_{k,i}}|A_{k,i}, Z_{k,i}\rangle$ and $e^{i\zeta_{k,f}}|A_{k,f}, Z_{k,f}\rangle$ the squeezed coherent state respectively at the beginning and at the end of the time interval t_k . The final state for each time interval coincides with the initial state for the following one:

$$e^{i\zeta_{k,i}}|A_{k,i}, Z_{k,i}\rangle \equiv e^{i\zeta_{k-1,f}}|A_{k-1,f}, Z_{k-1,f}\rangle \quad (50)$$

In order to derive the vibrational state at the end of the time interval, one can first reduce the time evolution operator to the product of squeeze, displacement, and rotation operators [Eq. (45)], and then sequentially apply such operators to the vibrational state. The resulting intermediate states, referred to as $e^{i\zeta_{k,l}}|A_{k,l}, Z_{k,l}\rangle$, are given by:

1. The first intermediate state is obtained by applying the squeeze operator, and thus Eqs. (40-44), with $W = X_0$. The states before and after such application are specified by $(A, Z, \zeta) = (A_{k,i}, Z_{k,i}, \zeta_{k,i})$ and $(A', Z', \zeta') = (A_{k,1}, Z_{k,1}, \zeta_{k,1})$.
2. The second intermediate state is obtained by applying a rotation operator, and thus Eqs. (36-37), with $\Phi = \Phi_{\lambda_k}$. The states before and after such application are specified by $(A, Z, \zeta) = (A_{k,1}, Z_{k,1}, \zeta_{k,1})$, $(A', Z', \zeta') = (A_{k,2}, Z_{k,2}, \zeta_{k,2})$.
3. The third intermediate state is obtained by applying a second squeeze operator, and thus results from Eqs. (40-44) with $W = -X_{\lambda_k}$. The states before and after such application are specified by $(A, Z, \zeta) = (A_{k,2}, Z_{k,2}, \zeta_{k,2})$, $(A', Z', \zeta') = (A_{k,3}, Z_{k,3}, \zeta_{k,3})$.
4. The fourth intermediate state is obtained by applying a displacement operator, whose effect on the squeezed coherent state is given by Eqs. (38-39), with $B = \Delta_{\lambda_k}$. The states before and after such application are specified by $(A, Z, \zeta) = (A_{k,3}, Z_{k,3}, \zeta_{k,3})$, $(A', Z', \zeta') = (A_{k,4}, Z_{k,4}, \zeta_{k,4})$.
5. The fifth intermediate state results from the application of a rotation operator, whose effect is given by Eqs. (36-37), with $\Phi = \Phi'_{\lambda_k}$. The states before and after such application are specified by $(A, Z, \zeta) = (A_{k,4}, Z_{k,4}, \zeta_{k,4})$, $(A', Z', \zeta') = (A_{k,5}, Z_{k,5}, \zeta_{k,5})$.
6. The sixth intermediate state is obtained by applying a displacement operator, and thus Eqs. (38-39), with $B = -\Delta_{\lambda_k}$. The states before and after such application are specified by $(A, Z, \zeta) = (A_{k,5}, Z_{k,5}, \zeta_{k,5})$, $(A', Z', \zeta') = (\alpha_{k,6}, z_{k,6}, \zeta_{k,6})$.

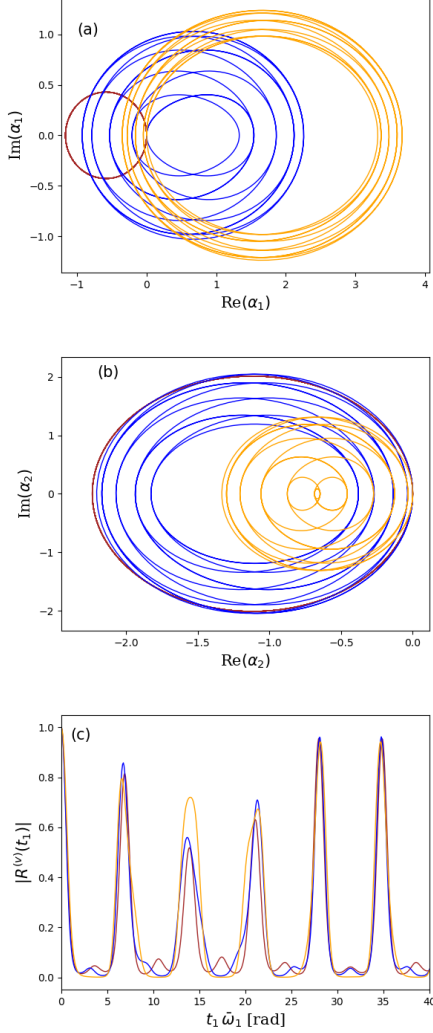


FIG. 5. Trajectory of the two-mode squeezed coherent state as a function of t_1 , defined by the values of (a) α_1 and (b) α_2 . Please note that for visualization purposes, the scales of the two axes are different. (c) Time dependence of the linear response function ($N = 1$), with $\bar{\omega}_1 \equiv (\omega_{1,1} + \omega_{1,2})/2$. The curves in the three panels are obtained for $\delta_{1,1} = 0.5$ and $\omega_{1,1}/\omega_{0,1} = 0.73$ (first mode), $\delta_{1,2} = 1.5$ and $\omega_{1,2}/\omega_{0,2} = 1.8$ (second mode). Curves of different colors correspond to different values of the rotation angle φ_1/π , and specifically: 0 (brown), 0.2 (blue), 0.4 (orange).

7. The seventh intermediate state results from the application of a squeeze operator [Eqs. (40-44)], with $W = X_{\lambda_k}$. The states before and after such application are specified by $(A, Z, \zeta) = (A_{k,6}, Z_{k,6}, \zeta_{k,6})$, $(A', Z', \zeta') = (A_{k,7}, Z_{k,7}, \zeta_{k,7})$.
8. The eighth intermediate state is obtained from the application of a rotation operator, and thus from Eqs. (36-37), with $\Phi = -\Phi_{\lambda_k}$. The states before and after such application are specified by $(A, Z, \zeta) = (A_{k,7}, Z_{k,7}, \zeta_{k,7})$, $(A', Z', \zeta') =$

$$(A_{k,8}, Z_{k,8}, \zeta_{k,8}).$$

9. The ninth intermediate state is obtained from a squeeze operator, and thus from Eqs. (40-44), with $W = -X_0$. The states before and after such application are specified by $(A, Z, \zeta) = (A_{k,8}, Z_{k,8}, \zeta_{k,8})$, $(A', Z', \zeta') = (A_{k,9}, Z_{k,9}, \zeta_{k,9})$.

The final state is finally obtained by modifying the phase factor, according to the equations $\alpha_{k,f} = \alpha_{k,9}$, $z_{k,f} = z_{k,9}$, and $\zeta_{k,f} = \zeta_{k,9} - \sum_{j=1}^N \omega_{\lambda_k,j} t_k/2$.

D. Vibrational response function

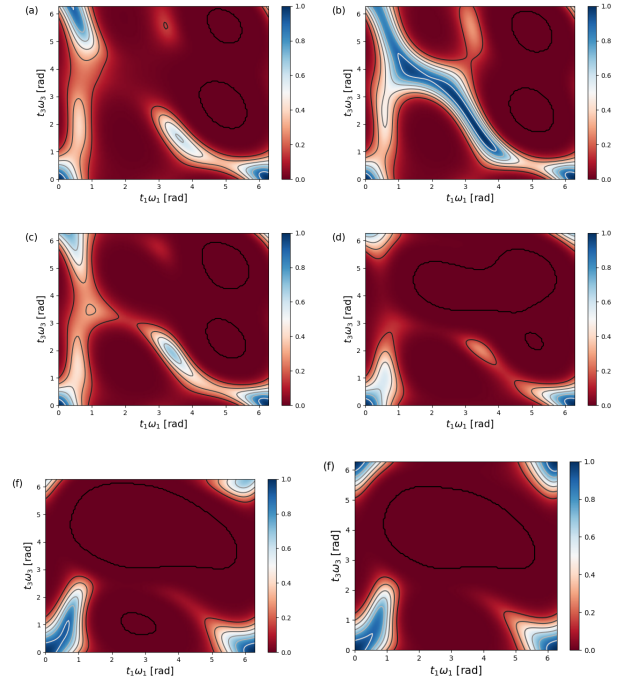


FIG. 6. Absolute value of the third-order ($M = 3$) vibrational response function $R^{(v)}$, as a function of the waiting times t_1 and t_3 , at $t_2\bar{\omega}_0 = 1.5\pi$. The plots are obtained for $\delta_{1,1} = 0.5$ and $\omega_{1,1}/\omega_{0,1} = 0.67$ (first mode), $\delta_{1,2} = 1.5$ and $\omega_{1,2}/\omega_{0,2} = 2$ (second mode). Different panels correspond to different values of the Duschinsky rotation angle φ_1/π , and specifically: (a) 0, (b) 0.1, (c) 0.2, (d) 0.3, (e) 0.4, (f) 0.5.

The vibrational component of the M -th order response function is given by the overlap between the final vibrational state and the initial ground state, i.e. to that between a vacuum and a squeezed coherent state [58]:

$$R_{\Lambda}^{(v,M)}(t_1, \dots, t_M) = e^{i\zeta} \langle 0|A, Z \rangle = e^{i\zeta} d_{S_Z}^{1/2} \exp \left[-\frac{1}{2} (A^\dagger A - A^\dagger T_Z A^*) \right] \quad (51)$$

where d_{S_Z} is the determinant of S_Z , while the squeezed coherent state is given by $A = A_{M,f}$, $Z = Z_{M,f}$, and $\zeta =$

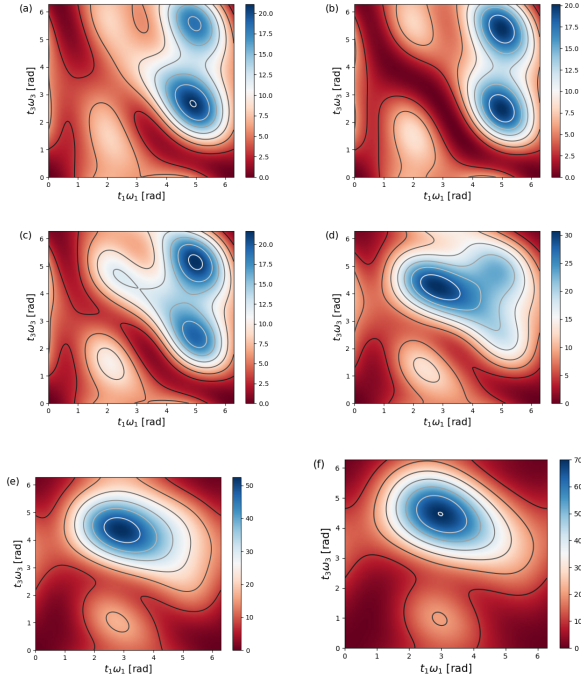


FIG. 7. Dependence of $|A|^2 = |\alpha_1|^2 + |\alpha_2|^2$ on the waiting times t_1 and t_3 , for $t_2\bar{\omega}_0 = 1.5\pi$. The plots are obtained for $\delta_{1,1} = 0.5$ and $\omega_{1,1}/\omega_{0,1} = 0.67$ (first mode), $\delta_{1,2} = 1.5$ and $\omega_{1,2}/\omega_{0,2} = 2$ (second mode). Different panels correspond to different values of the Duschinsky rotation angle, and specifically: φ_1/π : (a) 0, (b) 0.1, (c) 0.2, (d) 0.3, (e) 0.4, (f) 0.5.

$\zeta_{M,f} + \sum_{j=1}^N \omega_{0,j} \sum_{k=1}^M t_k/2$. As to the matrices, given the polar decomposition $Z = |Z|e^{i\Theta z}$, they are defined by the relations $T_Z = \tanh|Z|e^{i\Theta z}$ and $S_Z = \text{sech}|Z|$.

If the initial state of the vibrational modes is a generic squeezed coherent state, $|A_0, Z_0\rangle$, the derivation of the response function must include an additional rotation, squeeze and displacement operator. Equation (25) applies, as in the single-mode case, but the fictitious final state $|\psi'_{ket,\Lambda}\rangle$ is now given by

$$\begin{aligned} |\psi'_{ket,\Lambda}\rangle &= S_N(-Z_0) D_N(-A_0) R_N(\Phi_0) \\ &\left(e^{-iH_{v,\lambda_M} t_M/\hbar} \dots e^{-iH_{v,\lambda_1} t_1/\hbar} \right) |A_0, Z_0\rangle, \end{aligned} \quad (52)$$

where $\Phi_0 = \sum_{j=1}^M t_j \text{diag}(\omega_{0,1}, \dots, \omega_{0,N})$, and the product of time evolution operators in parentheses is reduced to the product of squeeze, displacement and rotation operators as shown above.

E. Application to some representative case

As an illustrative example, we apply the above results to the case of linear and nonlinear response functions for a system with two electronic levels ($N_e = 2$) and two vibrational modes ($N = 2$). Given the presence of only two vibrational modes, the Duschinsky matrix can be

expressed as a function of a single rotation angle [60]:

$$U_\lambda = \begin{pmatrix} \cos \varphi_\lambda & \sin \varphi_\lambda \\ -\sin \varphi_\lambda & \cos \varphi_\lambda \end{pmatrix}. \quad (53)$$

The corresponding rotation operator $R_2(\Phi_\lambda)$ is defined by the imaginary and Hermitian matrix

$$\Phi_\lambda = \begin{pmatrix} 0 & -i\varphi_\lambda \\ i\varphi_\lambda & 0 \end{pmatrix}. \quad (54)$$

Given the presence of only two electronic states, there is only one relevant rotation operator $R_2(\Phi_1)$, defined by the above expression, with a rotation angle φ_1 .

1. First order

In the linear case ($M = 1$), the electronic component of the response function is given by Eq. (27). The vibrational response function is obtained from the equations presented in this Section, for $M = 1$ and $\lambda_1 = 1$. In the absence of a rotation ($\varphi_1 = 0$), the final two-mode state is simply given by the product of two single-mode squeezed coherent states, and $R_\lambda^{(v,1)}(t_1)$ coincides with the product of the corresponding single-mode response functions. The trajectories described by α_1 and α_2 are periodic and independent from one another, with periods $2\pi/\omega_{1,1}$ and $2\pi/\omega_{1,2}$, respectively [Fig. 5(a,b), brown curves]. For $\varphi_1 \neq 0$, the Duschinsky rotation couples the two frequencies and complicates the trajectories, whose period now coincides with that of the overall rotation operator $R_2(\Phi_1)$. This is given by $T = 2k_1\pi/\omega_{1,1} = 2k_2\pi/\omega_{1,2}$, being k_1 and k_2 the smallest integers such that fulfil the second equality (in the reported example, $k_1 = 11$ and $k_2 = 9$, corresponding to $T\bar{\omega} = 20\pi$). If the frequencies $\omega_{1,1}$ and $\omega_{1,2}$ are not commensurate, then the trajectories described by the α_j in the respective planes are in general open.

The vibrational response function presents features that are qualitatively similar to those observed in the single-mode case, but with a longer period [Fig. 5(c)] or with no periodic behavior, depending on the ratio between the two excited-state frequencies $\omega_{1,j}$ ($j = 1, 2$). Comparing the time dependence of α_1 and α_2 with that of the response function's modulus, it emerges that its main maxima correspond to the times where both vibrational wave packets are close to the origin (*i.e.*, both α_1 and α_2 are close to zero). The lower maxima, instead, correspond to times where only one of the two wave packets is close to the origin.

2. Third-order

For the third-order term ($M = 3$), we specifically consider the non-rephasing part of the ground-state bleaching contribution [$\lambda_1 = \lambda_3 = 1$ and $\lambda_2 = 0$, Fig. 1(b)]. The electronic part of the response function is given in

Eq. (28). The vibrational response function is displayed in Fig. 6 for different values of the mixing angle φ_1 . Its periodicity in the waiting times t_1 and t_3 follows the same properties outlined above for the first-order response function. The mixing angle changes the functional dependence of the response function on the waiting times t_1 and t_3 . In analogy to what happens in the single-mode case, such dependence is clearly correlated to that of $|A|^2$ (Fig. 7), being $|A, Z\rangle$ the final state of the two vibrational modes. This results from the fact that the overlap between $|A, Z\rangle$ and the initial vibrational (ground) state, exponentially depends on the square modulus of A [see Eq. (51)]. Even though the combination of rotation, squeeze and displacement operators gives rise to nontrivial two-mode states, the connection between the vibrational response function and the position of the vibrational wave packets thus remains clear.

IV. CONCLUSIONS

In conclusion, we develop an approach for the calculation of the vibrational response functions to be applied in the simulation of multidimensional electronic spectroscopy. The approach applies to systems whose N (relevant) vibrational modes can be described as independent harmonic oscillators, whose frequencies and origin depend on the electronic state. Besides, the field is assumed to induce Franck-Condon transitions between electronic states, resulting in a mixing of the normal vibrational modes (Duschinsky rotations). The approach allows the explicit derivation of the squeezed coherent multi-mode vibrational state generated by the sequence of field-induced excitations and free-evolution periods, whose overlap with the initial state gives the vibrational response function. From both the formal and the numerical points of view, the calculation of the response function at given waiting times is obtained by applying simple iterative relations (nine for each time interval) to the three quantities that define the vibrational state: a complex N -dimensional vector A , a complex $N \times N$ matrix Z , and a real number ζ . This replaces the time integration of the Schrödinger equation or the Hamiltonian diagonalization, combined with the sum over infinite vibronic pathways, that are required in alternative approaches. From a physical point of view, the present allows the derivation of the vibrational state generated within each electronic pathway, thus relating a clear physical picture to the behavior of the vibrational response function.

ACKNOWLEDGMENTS

This work has been supported by the European Union's Horizon 2020 research and innovation programme under the Marie Skłodowska-Curie Grant Agreement No. 812992.

Appendix A: Properties of the response functions

The contributions to the response function related to each electronic pathway can be written in a factorized form. Also, vibrational response functions that involve the same sequence of electronic states but correspond to different kinds of pathways can be derived from one another by suitable redefinitions of the waiting times. These properties are demonstrated in the following two paragraphs.

a. Factorization of the response function. The third-order response function corresponds to the four-point correlation function reported in Eq. 4. Replacing each dipole operator with its expression in terms of the time-evolution operators, one obtains terms such as:

$$\begin{aligned} & \langle \mu(t_{123}) \mu(t_{12}) \mu(t_1) \mu \rho_0 \rangle \\ &= \langle 0 | U^\dagger(t_{123}) \mu U(t_3) \mu U(t_2) \mu U(t_1) \mu | 0 \rangle \\ &= (i/\hbar)^{-3} \sum_{\Lambda} R_{\Lambda}^{(e,3)} R_{\Lambda}^{(v,3)}, \end{aligned} \quad (\text{A1})$$

which specifically corresponds to the term in Eq. (4) where all the dipole operators act on the density operator from the left. The vector $\Lambda = (\lambda_1, \lambda_2, \lambda_3)$ specifies the electronic states obtained after the application to the ket of the first, second, and third dipole operator, respectively. The possibility of writing each term in the above sum in a factorized form results from the expression of the time evolution operator related to the Hamiltonian in Eq. (1):

$$U = \sum_{\lambda} U_{e,\lambda} \otimes U_{v,\lambda} = \sum_{\lambda} |\lambda\rangle \langle \lambda| e^{-i\epsilon_{\lambda} t/\hbar} \otimes e^{-iH_{v,\lambda} t/\hbar}. \quad (\text{A2})$$

In particular, the electronic component of the response function reads:

$$R_{\Lambda}^{(e,3)} = C_{\Lambda} e^{-i(\epsilon_{\lambda_3} t_3 + \epsilon_{\lambda_2} t_2 + \epsilon_{\lambda_1} t_1)/\hbar}, \quad (\text{A3})$$

where $C_{\Lambda} = (i/\hbar)^3 \mu_{\lambda_1 0} \mu_{\lambda_2 \lambda_1} \mu_{\lambda_3 \lambda_2} \mu_{0 \lambda_3}$. The vibrational component of the response function is given by:

$$\begin{aligned} R_{\Lambda}^{(v,3)} &= \langle 0_0 | U_{v,0}^\dagger(t_{123}) U_{v,\lambda_3}(t_3) U_{v,\lambda_2}(t_2) U_{v,\lambda_1}(t_1) | 0_0 \rangle \\ &= e^{it_{123}\omega_0/2} \langle 0_0 | U_{v,\lambda_3}(t_3) U_{v,\lambda_2}(t_2) U_{v,\lambda_1}(t_1) | 0_0 \rangle, \end{aligned} \quad (\text{A4})$$

where $|n_{\lambda}\rangle = |0_0\rangle$ is the ground state of the undisplaced harmonic oscillator.

b. Terms related to different processes. The contribution to the response function explicitly derived in the above paragraph corresponds to the case where all the dipole operators act on the left side of the density operator ρ_0 . In the case $\lambda_2 = 0$, this would be the non-rephasing component of a ground state bleaching contribution. Let's now consider, for example, the case where the dipole operators μ and $\mu(t_{12})$ in Eq. (4) act on the

right of ρ_0 :

$$\begin{aligned} \langle \mu(t_{123}) \mu(t_1) \rho_0 \mu(t_{12}) \rangle &= \langle \mu \mu(t_{12}) \mu(t_{123}) \mu(t_1) \rho_0 \rangle \\ &= \langle 0 | \mu U^\dagger(t_{12}) \mu U^\dagger(t_3) \mu U(t_{23}) \mu U(t_1) | 0 \rangle \\ &= (i/\hbar)^{-3} \sum_{\Lambda} R_{\Lambda, \Gamma}^{(e,3)} R_{\Lambda, \Gamma}^{(v,3)}, \end{aligned} \quad (\text{A5})$$

where in the first equation we have exploited the cyclic property of the trace. The vector $\Gamma = (L, R, L)$ specifies the side of the double-sided Feynman diagram where the first three interactions with the field take place (it is intended that, when the vector is omitted, all interactions take place on the left side). For $\lambda_2 = 0$, this would be the rephasing component of a stimulated emission contribution. Proceeding as in the previous paragraph, one obtains the following expression for the electronic component of the response function:

$$R_{\Lambda, \Gamma}^{(e,3)} = C_{\Lambda, \Gamma} e^{i(\epsilon_{\lambda_3} t_{12} + \epsilon_{\lambda_2} t_3 - \epsilon_{\lambda_1} t_{23})/\hbar}, \quad (\text{A6})$$

where $C_{\Lambda, \Gamma} = (i/\hbar)^3 \mu_{j0} \mu_{kj} \mu_{lk} \mu_{0l}$. The vibrational component of the response function is given by:

$$\begin{aligned} R_{\Lambda, \Gamma}^{(v,3)} &= \langle 0_0 | U_{v, \lambda_3}^\dagger(t_{12}) U_{v, \lambda_2}^\dagger(t_3) U_{v, \lambda_1}(t_{23}) U_{v, 0}(t_1) | 0_0 \rangle \\ &= e^{-it_1 \omega_0/2} \langle 0_0 | U_{v, \lambda_3}^\dagger(t_{12}) U_{v, \lambda_2}^\dagger(t_3) U_{v, \lambda_1}(t_{23}) | 0_0 \rangle. \end{aligned} \quad (\text{A7})$$

From a comparison between Eq. (A4) and Eq. (A7) it follows that

$$R_{\Lambda, \Gamma}^{(v,3)}(t_1, t_2, t_3) = R_{\Lambda}^{(v,3)}(t_{23}, -t_3, -t_{12}), \quad (\text{A8})$$

with $\Gamma = (L, R, L)$.

One can show that analogous relations can be established between contributions characterized by the same sequences of electronic states in the double-sided Feynman diagram, moving clockwise from the first state on the left (ket) to the last one on the right (bra). In all cases, for a generic Λ , you end up with a response function of the form

$$R_{\Lambda, \Gamma}^{(v,3)} = e^{it_{abc} \omega_0/2} \langle 0_0 | U_{v, \lambda_3}(t_c) U_{v, \lambda_2}(t_b) U_{v, \lambda_1}(t_a) | 0_0 \rangle,$$

where $t_{abc} = t_a + t_b + t_c$ and t_a, t_b, t_c are given by different combinations of t_1, t_2, t_3 [64].

Appendix B: Properties of the single-mode rotation, displacement, and squeeze operators

The time evolution generated by the vibrational Hamiltonians $H_{v, \lambda}$ [Eq. (2)] can be derived from the properties of the rotation, displacement, and squeeze operators [66], which are recalled hereafter.

a. Rotation operator. The rotation operator can be expressed as an exponential function of the number operator $n = a^\dagger a$:

$$R(\phi) = \exp(i\phi a^\dagger a), \quad (\text{B1})$$

where ϕ is real and defines the rotation angle. It's a unitary operator, whose inverse is given by:

$$R^{-1}(\phi) = R^\dagger(\phi) = R(-\phi). \quad (\text{B2})$$

Finally, the product of two rotations is still a rotation operator:

$$R(\phi_1) R(\phi_2) = R(\phi_3), \quad (\text{B3})$$

where $\phi_3 = \phi_1 + \phi_2$.

b. Displacement operator. The displacement operator is defined can be written as an exponential function of the creation and annihilation operators:

$$D(\alpha) = \exp(\alpha a^\dagger - \alpha^* a), \quad (\text{B4})$$

where α is a complex number. The displacement operator is unitary, and its inverse is given by:

$$D^{-1}(\alpha) = D^\dagger(\alpha) = D(-\alpha). \quad (\text{B5})$$

The product of two displacement operators is still a displacement operator, times a phase factor:

$$D(\alpha_1) D(\alpha_2) = e^{(\alpha_1 \alpha_2^* - \alpha_1^* \alpha_2)/2} D(\alpha_1 + \alpha_2). \quad (\text{B6})$$

c. Squeeze operator. The squeeze operator is given by an exponential function of the creation and annihilation operators squared:

$$S(z) = \exp\left\{\frac{1}{2}\left[z^* a^2 - z (a^\dagger)^2\right]\right\}, \quad (\text{B7})$$

where z is a complex number. This operator is also unitary, and its inverse is given by:

$$S^{-1}(z) = S^\dagger(z) = S(-z). \quad (\text{B8})$$

Finally, the product of two squeeze operators corresponds to that of a squeeze and a rotation operator:

$$S(z_1) S(z_2) = e^{i\phi/2} S(z_3) R(\phi) \quad (\text{B9})$$

where $z_j \equiv |z_j| e^{i\theta_j}$ and $(j = 1, 2, 3)$. The final squeezing parameters and rotation angle are defined by

$$t_3 = \frac{t_1 + t_2}{1 + t_2 t_1^*}, \quad e^{i\phi} = \frac{1 + t_1 t_2^*}{|1 + t_1 t_2^*|}, \quad (\text{B10})$$

with $t_j \equiv e^{i\theta_j} \tanh |z_j|$.

d. Commutation relations. Rotation, displacement, and squeeze operators don't commute with each other. This can be deduced from the effect of these transformations on the annihilation operator, which is given by the following equations:

$$R(-\phi) a R(\phi) = a e^{i\phi} \quad (\text{B11})$$

$$S(-z) a S(z) = a \cosh |z| - a^\dagger e^{i\theta} \sinh |z| \quad (\text{B12})$$

$$D(-\alpha) a D(\alpha) = a + \alpha \quad (\text{B13})$$

Combining the above equations with the definitions of the displacement, rotation, and squeeze operators, one obtains the expressions:

$$D(\alpha) R(\phi) = R(\phi) D(\alpha e^{-i\phi}) \quad (\text{B14})$$

$$S(z) R(\phi) = R(\phi) S(z e^{-i2\phi}) \quad (\text{B15})$$

$$S(z) D(\alpha) = D(\alpha \cosh |z| - \alpha^* e^{i\theta} \sinh |z|) S(z). \quad (\text{B16})$$

e. Application to the squeezed coherent states. From the above combination and commutation relations it follows that the application of a rotation, displacement, or squeeze operator to a squeezed coherent state produces another squeezed coherent state.

Let's start by considering the application of a rotation operator. This gives:

$$\begin{aligned} R(\phi) |\alpha, z\rangle &= D(e^{i\phi}\alpha) R(\phi) S(z) |0\rangle = \\ D(e^{i\phi}\alpha) S(e^{2i\phi}z) |0\rangle &= |e^{i\phi}\alpha, e^{2i\phi}z\rangle. \end{aligned} \quad (\text{B17})$$

As to the displacement operator, by applying the combination of the displacement operators, one obtains:

$$\begin{aligned} D(\beta) |\alpha, z\rangle &= e^{(\alpha^*\beta - \alpha\beta^*)/2} D(\alpha + \beta) S(z) |0\rangle \\ &= e^{(\alpha^*\beta - \alpha\beta^*)/2} |\alpha + \beta, z\rangle. \end{aligned} \quad (\text{B18})$$

Finally, the application of a squeeze operator to a squeezed coherent state is given by the equation:

$$S(w) |\alpha, z\rangle = D(\beta) S(w) S(z) |0\rangle = e^{i\phi/2} |\beta, u\rangle, \quad (\text{B19})$$

where

$$\beta = \alpha \cosh |w| - \alpha^* e^{i\theta_z} \sinh |w| \quad (\text{B20})$$

and

$$t_u = \frac{t_w + t_z}{1 + t_w^* t_z}, \quad e^{i\phi} = \frac{1 + t_w t_z^*}{|1 + t_w t_z^*|}. \quad (\text{B21})$$

Appendix C: Properties of the multi-mode rotation, displacement, and squeeze operators

The time evolution generated by the vibrational Hamiltonians $H_{v,\lambda}$ [Eq. (30)] can be derived from the properties of the multimode rotation, displacement, and squeeze operators [59], which are recalled hereafter.

a. Rotation operator. The rotation operator can be expressed as an exponential function of the vectorial creation and annihilation operators, $\tilde{a} = (a_1, \dots, a_N)$ and $\tilde{a}^\dagger = (a_1^\dagger, \dots, a_N^\dagger)$ (the tilde denotes the transposition of the matricial operator):

$$R_N(\Phi) = \exp(i\tilde{a}^\dagger \Phi a), \quad (\text{C1})$$

where Φ is a Hermitian matrix. It's a unitary operator, whose inverse is given by:

$$R_N^{-1}(\Phi) = R_N^\dagger(\Phi) = R_N(-\Phi). \quad (\text{C2})$$

Finally, the product of two rotations is still a rotation operator:

$$R_N(\Phi_1) R_N(\Phi_2) = R_N(\Phi_3), \quad (\text{C3})$$

where $e^{i\Phi_3} = e^{i\Phi_1} e^{i\Phi_2}$.

b. Displacement operator. The displacement operator can be written as an exponential function of the creation and annihilation operators:

$$D_N(A) = \exp(\tilde{A}a^\dagger - A^\dagger a), \quad (\text{C4})$$

where $\tilde{A} = (\alpha_1, \dots, \alpha_N)$ and $A^\dagger = (\alpha_1^*, \dots, \alpha_N^*)$ are a complex vectors (the tilde and the dagger applied to a numerical matrix denote its simple and conjugate transpositions, respectively). The displacement operator is unitary, and its inverse is given by:

$$D_N^{-1}(A) = D_N^\dagger(A) = D_N(-A). \quad (\text{C5})$$

The product of two displacement operators is still a displacement operator, times a phase factor:

$$D_N(A_1) D_N(A_2) = e^{(A_2^\dagger A_1 - A_1^\dagger A_2)/2} D_N(A_1 + A_2), \quad (\text{C6})$$

where $A_i^\dagger A_j$ are matrix products, whose result corresponds to scalars.

c. Squeeze operator. The squeeze operator is given by an exponential function of the creation and annihilation operators squared:

$$S_N(Z) = \exp\left[\frac{1}{2}(\tilde{a}Z^\dagger a - \tilde{a}^\dagger Z a)\right], \quad (\text{C7})$$

where Z is a symmetric matrix. This operator is also unitary, and its inverse reads:

$$S_N^{-1}(Z) = S_N^\dagger(Z) = S_N(-Z). \quad (\text{C8})$$

Finally, the product of two squeeze operators corresponds to that of a squeeze and a rotation operator:

$$S_N(Z_1) S_N(Z_2) = e^{\frac{i}{2}\text{Tr}(\Phi)} S_N(Z_3) R_N(\Phi) \quad (\text{C9})$$

where $Z_j \equiv |Z_j| e^{i\Theta_j}$ ($j = 1, 2, 3$), $|Z_j| = \sqrt{Z_j^\dagger Z_j}$, and

$$T_3 = S_1^{-1}(T_1 + T_2)(I + T_1^\dagger T_2)^{-1} \tilde{S}_1 \quad (\text{C10})$$

$$e^{i\Phi} = S_3^{-1} S_1(I + T_2 T_1^\dagger)^{-1} S_2 \quad (\text{C11})$$

being $T_j \equiv \tanh |Z_j| e^{i\Theta}$ and $S_j = \text{sech } |Z_j|$.

d. Commutation relations. Rotation, displacement, and squeeze operators don't commute with each other. This can be deduced from the effect of these transformations on the vectorial annihilation operator, which is given by the following equations

$$R_N(-\Phi) a R_N(\Phi) = e^{i\Phi} a \quad (\text{C12})$$

$$S_N(-Z) a S_N(Z) = \cosh |Z| a - \sinh |Z| e^{i\Theta} a^\dagger \quad (\text{C13})$$

$$D_N(-A) a D_N(A) = a + A. \quad (\text{C14})$$

Combining the above equations with the definitions of the displacement, rotation, and squeeze operators, one obtains the expressions:

$$D_N(A) R_N(\Phi) = R_N(\Phi) D(e^{-i\Phi} A) \quad (\text{C15})$$

$$S_N(Z) R_N(\Phi) = R_N(\Phi) S_N(e^{-i\Phi} Z e^{-i\Phi}) \quad (\text{C16})$$

$$S_N(Z) D_N(A) = D_N(\cosh |Z| A - \sinh |Z| e^{i\Theta} A^*) S_N(Z). \quad (\text{C17})$$

e. Application to the squeezed coherent states. From the above combination and commutation relations it follows that the application of a rotation, displacement, or squeeze operator to a squeezed coherent state produces another squeezed coherent state.

Let's start by considering the application of a rotation operator. This gives:

$$R_N(\Phi) |A, Z\rangle = D_N(e^{i\Phi} A) R_N(\Phi) S_N(Z) |0\rangle = D_N(e^{i\Phi} A) S_N(e^{i\Phi} Z e^{i\tilde{\Phi}}) |0\rangle = |e^{i\Phi} A, e^{i\Phi} Z e^{i\tilde{\Phi}}\rangle. \quad (\text{C18})$$

As to the displacement operator, by applying the com-

bination of the displacement operators, one obtains:

$$D_N(B) |A, Z\rangle = e^{(A^\dagger B - B^\dagger A)/2} D_N(A + B) S_N(Z) |0\rangle = e^{(A^\dagger B - B^\dagger A)/2} |A + B, Z\rangle. \quad (\text{C19})$$

Finally, the application of a squeeze operator to a squeezed coherent state is given by the equation:

$$S_N(W) |A, Z\rangle = D_N(B) S_N(W) S_N(Z) |0\rangle = e^{\frac{i}{2} \text{Tr}(\Phi)} |B, U\rangle. \quad (\text{C20})$$

where

$$B = \cosh |W| A - \sinh |W| e^{i\theta W} A^* \quad (\text{C21})$$

and

$$T_U = S_W^{-1} (T_W + T_Z) (I + T_W^\dagger T_Z)^{-1} \tilde{S}_W \quad (\text{C22})$$

$$e^{i\Phi} = S_U^{-1} S_W (I + T_Z T_W^\dagger)^{-1} S_Z. \quad (\text{C23})$$

-
- [1] P. Hamm and M. T. Zanni, *Concepts and Methods of 2D Infrared Spectroscopy* (Cambridge University Press, 2011).
- [2] M. Maiuri, M. Garavelli, and G. Cerullo, Ultrafast spectroscopy: State of the art and open challenges, *Journal of the American Chemical Society* **142**, 3 (2020).
- [3] S. Mukamel, *Principles of Nonlinear Optical Spectroscopy* (Oxford University Press, 1995).
- [4] S. Biswas, J. Kim, X. Zhang, and G. D. Scholes, Coherent two-dimensional and broadband electronic spectroscopies, *Chemical Reviews* **122**, 4257 (2022).
- [5] J. T. Kennis and M.-L. Groot, Ultrafast spectroscopy of biological photoreceptors, *Current opinion in structural biology* **17**, 623 (2007).
- [6] N. Christensson, H. F. Kauffmann, T. Pullerits, and T. Mančal, Origin of long-lived coherences in light-harvesting complexes, *The Journal of Physical Chemistry B* **116**, 7449 (2012).
- [7] J. Lloyd-Hughes, P. M. Oppeneer, T. P. Dos Santos, A. Schleife, S. Meng, M. A. Sentef, M. Ruggenthaler, A. Rubio, I. Radu, M. Murnane, *et al.*, The 2021 ultrafast spectroscopic probes of condensed matter roadmap, *Journal of Physics: Condensed Matter* **33**, 353001 (2021).
- [8] R. Croce, R. Van Grondelle, H. Van Amerongen, and I. Van Stokkum, *Light harvesting in photosynthesis* (CRC press, 2018).
- [9] L. Moretti, B. Kudisch, Y. Terazono, A. L. Moore, T. A. Moore, D. Gust, G. Cerullo, G. D. Scholes, and M. Maiuri, Ultrafast dynamics of nonrigid zinc-porphyrin arrays mimicking the photosynthetic “special pair”, *The Journal of Physical Chemistry Letters* **11**, 3443 (2020).
- [10] A. De Sio, F. Troiani, M. Maiuri, J. Réhault, E. Sommer, J. Lim, S. F. Huelga, M. B. Plenio, C. A. Rozzi, G. Cerullo, E. Molinari, and C. Lienau, Tracking the coherent generation of polaron pairs in conjugated polymers, *Nature Communications* **7**, 13742 (2016).
- [11] J. Cao, R. J. Cogdell, D. F. Coker, H.-G. Duan, J. Hauer, U. Kleinekathöfer, T. L. C. Jansen, T. Mančal, R. J. D. Miller, and J. P. Ogilvie, Quantum biology revisited, *Sci. Adv.* **6**, eaaz4888 (2020).
- [12] S. Rafiq, B. Fu, B. Kudisch, and G. D. Scholes, Interplay of vibrational wavepackets during an ultrafast electron transfer reaction, *Nat. Chem.* **13**, 70 (2021).
- [13] A. Anda, D. Abramavičius, and T. Hansen, Two-dimensional electronic spectroscopy of anharmonic molecular potentials, *Physical Chemistry Chemical Physics* **20**, 1642 (2018).
- [14] R. B. Weakly, J. D. Gaynor, and M. Khalil, Multimode two-dimensional vibronic spectroscopy. ii. simulating and extracting vibronic coupling parameters from polarization-selective spectra, *J. Chem. Phys.* **154**, 184202 (2021).
- [15] H.-D. Zhang, Q. Qiao, R.-X. Xu, and Y. Yan, Effects of Herzberg–Teller vibronic coupling on coherent excitation energy transfer, *The Journal of Chemical Physics* **145**, 204109 (2016).
- [16] L. A. Bizimana, W. P. Carbery, T. A. Gellen, and D. B. Turner, Signatures of Herzberg–Teller coupling in three-dimensional electronic spectroscopy, *J. Chem. Phys.* **146**, 084311 (2017).
- [17] S. Kundu, P. P. Roy, G. R. Fleming, and N. Makri, Franck–Condon and Herzberg–Teller signatures in molecular absorption and emission spectra, *The Journal of Physical Chemistry B* **126**, 2899 (2022).
- [18] O. Kühn, 8 - frenkel exciton dynamics: A theoretical perspective, in *Handbook of Organic Materials for Electronic and Photonic Devices (Second Edition)*, Woodhead Publishing Series in Electronic and Optical Materials, edited by O. Ostroverkhova (Woodhead Publishing, 2019) pp. 259–279.
- [19] R. Y. Prasad *et al.*, *Computational Quantum Chemistry* (CRC Press, 2021).
- [20] D. Young, *Computational chemistry: a practical guide for applying techniques to real world problems* (John Wiley

- & Sons, 2004).
- [21] T. Begušić and J. Vaníček, Finite-temperature, anharmonicity, and Duschinsky effects on the two-dimensional electronic spectra from ab initio thermo-field gaussian wavepacket dynamics, *The Journal of Physical Chemistry Letters* **12**, 2997 (2021).
- [22] A. F. Fidler and G. S. Engel, Nonlinear spectroscopic theory of displaced harmonic oscillators with differing curvatures: A correlation function approach, *The Journal of Physical Chemistry A* **117**, 9444 (2013).
- [23] T. J. Zuehlsdorff, H. Hong, L. Shi, and C. M. Isborn, Nonlinear spectroscopy in the condensed phase: The role of Duschinsky rotations and third order cumulant contributions, *J. Chem. Phys.* **153**, 044127 (2020).
- [24] T. Mančal, A. Nemeth, F. Milota, V. Lukeš, H. F. Kauffmann, and J. Sperling, Vibrational wave packet induced oscillations in two-dimensional electronic spectra. ii. theory, *The Journal of Chemical Physics* **132**, 184515 (2010).
- [25] H. Seiler, S. Palato, C. Sonnichsen, H. Baker, E. Socie, D. P. Strandell, and P. Kambhampati, Two-dimensional electronic spectroscopy reveals liquid-like lineshape dynamics in CsPbI₃ perovskite nanocrystals, *Nature communications* **10**, 1 (2019).
- [26] K. Shen, K. Sun, and Y. Zhao, Simulation of emission spectra of transition metal dichalcogenide monolayers with the multimode brownian oscillator model, *The Journal of Physical Chemistry A* **126**, 2706 (2022).
- [27] H.-P. Breuer and F. Petruccione, *The theory of open quantum systems* (Oxford University Press, 2002).
- [28] V. Butkus, D. Zigmantas, L. Valkunas, and D. Abramavicius, Vibrational vs. electronic coherences in 2d spectrum of molecular systems, *Chemical Physics Letters* **545**, 40 (2012).
- [29] J. A. Cina, P. A. Kovac, C. C. Jumper, J. C. Dean, and G. D. Scholes, Ultrafast transient absorption revisited: Phase-flips, spectral fingers, and other dynamical features, *J. Chem. Phys.* **144**, 175102 (2016).
- [30] D. V. Le, X. Leng, and H.-S. Tan, Regarding expressions of the oscillatory patterns in the 2d spectra of a displaced oscillator model, *Chemical Physics* **546**, 111142 (2021).
- [31] A. F. Fidler and G. S. Engel, Nonlinear spectroscopic theory of displaced harmonic oscillators with differing curvatures: A correlation function approach, *J. Phys. Chem. A* **117**, 9444 (2013).
- [32] E. Doktorov, I. Malkin, and V. Man'ko, Dynamical symmetry of vibronic transitions in polyatomic molecules and the Franck-Condon principle, *Journal of Molecular Spectroscopy* **64**, 302 (1977).
- [33] J. R. Caram, A. F. Fidler, and G. S. Engel, Excited and ground state vibrational dynamics revealed by two-dimensional electronic spectroscopy, *J. Chem. Phys.* **137**, 024507 (2012).
- [34] L. D. Smith, *Modelling quantum dynamics in molecular photoswitches*, Ph.D. thesis, University of Leeds (2021).
- [35] Z. L. Pianowski, Recent implementations of molecular photoswitches into smart materials and biological systems, *Chemistry—A European Journal* **25**, 5128 (2019).
- [36] G. M. Sando, K. G. Spears, J. T. Hupp, and P. T. Ruhoff, Large electron transfer rate effects from the Duschinsky mixing of vibrations, *The Journal of Physical Chemistry A* **105**, 5317 (2001).
- [37] J. Tang, M. T. Lee, and S. H. Lin, Effects of the Duschinsky mode-mixing mechanism on temperature dependence of electron transfer processes, *The Journal of Chemical Physics* **119**, 7188 (2003).
- [38] Q. Peng, Y. Yi, Z. Shuai, and J. Shao, Excited state radiationless decay process with Duschinsky rotation effect: Formalism and implementation, *The Journal of Chemical Physics* **126**, 114302 (2007).
- [39] B. de Souza, F. Neese, and R. Izsák, On the theoretical prediction of fluorescence rates from first principles using the path integral approach, *The Journal of Chemical Physics* **148**, 034104 (2018).
- [40] Y. Niu, Q. Peng, C. Deng, X. Gao, and Z. Shuai, Theory of excited state decays and optical spectra: Application to polyatomic molecules, *The Journal of Physical Chemistry A* **114**, 7817 (2010).
- [41] R. Ianculescu and E. Pollak, Photoinduced cooling of polyatomic molecules in an electronically excited state in the presence of Dushinskii rotations, *The Journal of Physical Chemistry A* **108**, 7778 (2004).
- [42] P. C. Arpin, M. Popa, and D. B. Turner, Signatures of Duschinsky rotation in femtosecond coherence spectra, *AppliedMath* **2**, 675 (2022).
- [43] T. L. Courtney, Z. W. Fox, K. M. Slenkamp, and M. Khalil, Two-dimensional vibrational-electronic spectroscopy, *The Journal of Chemical Physics* **143**, 154201 (2015).
- [44] G. Fumero, C. Schnederermann, G. Batignani, T. Wende, M. Liebel, G. Bassolino, C. Ferrante, S. Mukamel, P. Kukura, and T. Scopigno, Two-dimensional impulsively stimulated resonant Raman spectroscopy of molecular excited states, *Phys. Rev. X* **10**, 011051 (2020).
- [45] A. Baiardi, J. Bloino, and V. Barone, General time dependent approach to vibronic spectroscopy including Franck-Condon, Herzberg-Teller, and Duschinsky effects, *Journal of Chemical Theory and Computation* **9**, 4097 (2013).
- [46] J.-L. Chang, A new method to calculate Franck-Condon factors of multidimensional harmonic oscillators including the Duschinsky effect, *The Journal of Chemical Physics* **128**, 174111 (2008).
- [47] T. Sattasathuchana, J. S. Siegel, and K. K. Baldrige, Generalized analytic approach for determination of multidimensional Franck-Condon factors: Simulated photoelectron spectra of polynuclear aromatic hydrocarbons, *Journal of Chemical Theory and Computation* **16**, 4521 (2020).
- [48] J. Sung and R. J. Silbey, Four wave mixing spectroscopy for a multilevel system, *The Journal of Chemical Physics* **115**, 9266 (2001).
- [49] J. Sung and R. J. Silbey, Optical four wave mixing spectroscopy for multilevel systems coupled to multimode brownian oscillators, *The Journal of Chemical Physics* **118**, 2443 (2003).
- [50] T. J. Zuehlsdorff, A. Montoya-Castillo, J. A. Napoli, T. E. Markland, and C. M. Isborn, Optical spectra in the condensed phase: Capturing anharmonic and vibronic features using dynamic and static approaches, *The Journal of Chemical Physics* **151**, 074111 (2019).
- [51] T. J. Zuehlsdorff, S. V. Shedge, S.-Y. Lu, H. Hong, V. P. Aguirre, L. Shi, and C. M. Isborn, Vibronic and environmental effects in simulations of optical spectroscopy, *Annual Review of Physical Chemistry* **72**, 165 (2021).
- [52] C. A. Rozzi, F. Troiani, and I. Tavernelli, Quantum modeling of ultrafast photoinduced charge separation, *Journal of Physics: Condensed Matter* **30**, 013002 (2018).
- [53] S. A. Shah, H. Li, E. R. Bittner, C. Silva, and A. Piryatin-

- ski, Qudpy: A python-based tool for computing ultrafast non-linear optical responses (2022), [arXiv:2210.16355](https://arxiv.org/abs/2210.16355) [quant-ph].
- [54] P. A. Rose and J. J. Krich, Efficient numerical method for predicting nonlinear optical spectroscopies of open systems, *The Journal of Chemical Physics* **154**, 034108 (2021).
- [55] P. A. Rose and J. J. Krich, Automatic feynman diagram generation for nonlinear optical spectroscopies and application to fifth-order spectroscopy with pulse overlaps, *The Journal of Chemical Physics* **154**, 034109 (2021).
- [56] M. F. Gelin, L. Chen, and W. Domcke, Equation-of-motion methods for the calculation of femtosecond time-resolved 4-wave-mixing and n-wave-mixing signals, *Chemical Reviews* (2022).
- [57] A. Jain, A. S. Petit, J. M. Anna, and J. E. Subotnik, Simple and efficient theoretical approach to compute 2D optical spectra, *The Journal of Physical Chemistry B* **123**, 1602 (2019).
- [58] X. Ma and W. Rhodes, Squeezing in harmonic oscillators with time-dependent frequencies, *Phys. Rev. A* **39**, 1941 (1989).
- [59] X. Ma and W. Rhodes, Multimode squeeze operators and squeezed states, *Phys. Rev. A* **41**, 4625 (1990).
- [60] E. Doktorov, I. Malkin, and V. Man'ko, Dynamical symmetry of vibronic transitions in polyatomic molecules and the Franck-Condon principle, *Journal of Molecular Spectroscopy* **56**, 1 (1975).
- [61] J. Huh, G. G. Guerreschi, B. Peropadre, J. R. McClean, and A. Aspuru-Guzik, Boson sampling for molecular vibronic spectra, *Nature Photonics* **9**, 615 (2015).
- [62] F. E. Quintela Rodriguez and F. Troiani, Vibrational response functions for multidimensional electronic spectroscopy in the adiabatic regime: A coherent-state approach, *The Journal of Chemical Physics* **157**, 034107 (2022).
- [63] Y. Tanimura and S. Mukamel, Real-time path-integral approach to quantum coherence and dephasing in nonadiabatic transitions and nonlinear optical response, *Phys. Rev. E* **47**, 118 (1993).
- [64] F. Troiani, Vibrational response functions for multidimensional electronic spectroscopy in nonadiabatic models, *The Journal of Chemical Physics* **158** (2023), 054110.
- [65] C. Gerry and P. Knight, *Introductory Quantum Optics* (Cambridge University Press, Cambridge, 2004).
- [66] M. O. Scully and M. S. Zubairy, *Quantum Optics* (Cambridge University Press, 1997).